

Statistical Analysis and Optimization of Factors Affecting the Surface Roughness in the UVaSPIF Process Using Response Surface Methodology

M. Vahdati^{a,*}, R. A. Mahdavinejad^a, S. Amini^b, M. Moradi^c

^a Department of Mechanical Engineering, University of Tehran, Tehran, Iran.

^b Department of Mechanical Engineering, University of Kashan, Kashan, Iran.

^c Department of Mechanical Engineering, Malayer University, Malayer, Iran.

ARTICLE INFO

Article history:

Received 12 September 2014

Accepted 18 January 2015

Available online 15 March 2015

Keywords:

Single Point Incremental Forming
Ultrasonic Vibration
Surface Roughness
Response Surface Methodology

ABSTRACT

Ultrasonic vibration assisted single point incremental forming (UVaSPIF) is based on localized plastic deformation in a sheet metal blank. It consists of deforming gradually and locally the sheet metal using vibrating hemispherical-head tool controlled by a CNC milling machine. The ultrasonic excitation of the forming tool reduces the vertical component of the forming force. In addition, application of ultrasonic vibration reduces the surface roughness of the specimen. Surface roughness is one of the quantitative and qualitative parameters, which is used to assess the quality of the final product. In the present paper, a statistical analysis and optimization of the effective factors on this parameter are performed in the UVaSPIF process. For this purpose, response surface methodology (RSM) is selected as the experiment design technique. The controllable factors such as vertical step size, sheet thickness, tool diameter, wall inclination angle, and feed rate are specified as input variables of the process. The obtained results from the analysis of variance (ANOVA) and regression analysis of the experimental data confirm the accuracy of the mathematical model. Furthermore, it is shown that the linear, quadratic, and interactional terms of the variables are effective on the surface roughness parameter. To optimize the surface roughness parameter, the most appropriate conditions of the experiment are determined using desirability method, and statistical optimization is subsequently verified by conducting the confirmation test.

1. Introduction

Nowadays, sheet metal-forming industries need to use economical and flexible processes to meet the market demands in a competitive environment with a minimum cost and time. Thus, researchers have considered the investigation of operational methods in order to produce and develop the new products[1-4].

Single point incremental forming (SPIF) has been introduced as an attractive and flexible method among the rapid prototyping processes with a high potential to be produced in a small volume. Leszak [5] patented this process in 1967 and its feasibility was confirmed by Kitazawa et al. [6] in forming of rotational symmetric parts. In this process, a simple

Corresponding author:

E-mail address: vahdati@ut.ac.ir (Mehdi Vahdati).

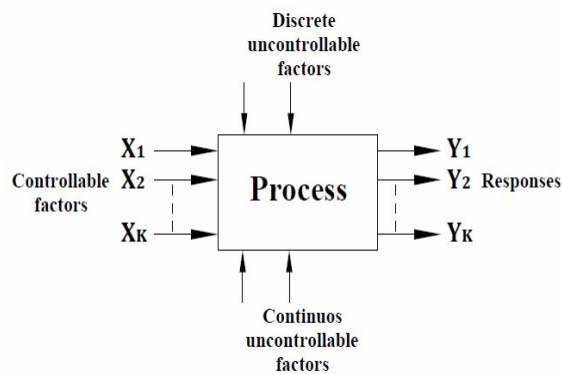


Fig. 1. General model of the process

forming tool with hemispherical-head moves on a sheet metal in a programmed path and applies local plastic deformation to create the final geometry [7-10].

The surface finish of the formed sample in incremental forming has a lower situation compared with other forming processes [11, 12]. Thus, in order to predict and control this parameter in incremental forming, researchers have considered the investigation of the surface roughness parameter. Junk et al. [13] observed that with the increase of vertical step size, the surface roughness increases and with the increase of tool diameter and wall inclination angle, the surface roughness decreases. Hagan and Jeswiet [14] studied the significance of the surface roughness in a microscopic scale in particular in relation to the automobile components. They described the surface finish in incremental forming in the form of a combination of wave state in large scale (resulting from tool path) and roughness in a small scale (resulting from large plain strains). It was shown that, as the vertical step size decreases, the surfaces are seen to transform from wavy to strictly rough without waviness. They also reported that the spindle speed has no effect on the surface roughness. Durante et al. [15] presented the theoretical model of the surface roughness in form of the following relation:

$$R_z = \frac{315.25v^2}{d^1.43 \sin^2\phi} \quad [1]$$

In this relation, R_z is the surface roughness parameter. As can be observed, the reduction of vertical step size (v), the increase of tool

diameter (d) and the increase of wall inclination angle (ϕ) lead to the reduction of the surface roughness parameter. Shanmuganatan and Kumar [16] also found that the increase of wall inclination angle and tool diameter reduces the surface roughness parameter.

Vahdati et al. [17, 18] showed that ultrasonic excitation of the hemispherical-head tool in SPIF reduces the vertical component of the forming force and surface roughness of the specimen. Thus, the sheet metal will be formed incrementally in the presence of ultrasonic vibration with given frequency and specified amplitude as compared to previous researches. Hence, in the present paper, the analysis and optimization of surface roughness in UVaSPIF is done based on the DOE principles using the RSM technique. Design of experiments specially RSM is widely used for modeling and optimization of the production processes, such as welding, powder metallurgy, casting, and so on [19, 20]. The objectives of this research include extraction of regression model and mathematical equation resulting from ANOVA for surface roughness parameter and access to optimal conditions of the experiment.

2. Experimental

Fig. 1. shows the general model of the process. Assuming the independence of controllable factors (X_i) and response of the process (Y_i), the goal is to obtain the mathematical relation between the output and the input variables with minimum error. For this purpose, the methodology of statistical analysis in this research includes the following seven steps:

- Selecting the response variable
- Selecting the controllable factors
- Selecting the experiment design
- Experiment execution
- Measuring the response variable
- Data analysis
- Optimization and confirmation

2.1. Selecting the response variable

In order to evaluate the surface roughness of the specimen, the parameter of R_z was

Table 1. Input variables with design levels

Variable	Notation	Unit	-1	0	+1
Vertical step size	v	mm	0.25	0.5	0.75
Sheet thickness	t	mm	0.4	0.7	1
Tool diameter	d	mm	10	15	20
Wall inclination angle	φ	°	40	50	60
Feed rate	f	mm/min	1500	2000	2500

considered as a criterion to measure the surface roughness. R_z is the average peak to valley height of the profile. It was selected to prevent the influence of any accidental surface irregularity on the experimental evaluation of roughness.

2. 2. Selecting the controllable factors

During the UVaSPIF process, the applied force on the tool leads to the change in the vibration conditions. Therefore, vibration parameters such as frequency and amplitude of vibration were considered as the uncontrollable factors.

Thus, the five factors of vertical step size (**v**), sheet thickness (**t**), tool diameter (**d**), wall inclination angle (**φ**) and feed rate (**f**) were selected as the controllable input variables and each of them were considered at three levels of low (-1), central (0), and high (+1). The high and low levels of each parameter are coded by +1 and -1. The coded value of each intermediate level is calculated through the following relation [21]:

$$X = \frac{2x - (x_{\max} + x_{\min})}{(x_{\max} - x_{\min})} \quad [2]$$

In this relation, X is the coded value of concerned parameter with the actual value of **x** (between x_{\min} and x_{\max}). x_{\min} and x_{\max} have the actual low and high values of the parameter, accordingly. Table 1 shows the input variables and experimental design levels used with coded and actual values. The variation range of these factors was determined based on the primary experiments, which lead to safe production of the specimen.

2. 3. Selecting the experiment design

In the present research, RSM is used as the experiment design technique [22, 23]. Thus, the first step in this method is to find a suitable

approximation of the real relation existing between the response variable (**y**) and the set of input variables (**x**). The approximating functions are in the form of linear and quadratic models and are written in the form of the following relations:

$$y = \beta_0 + \beta_1 x_1 + \beta_2 x_2 + \dots + \beta_k x_k + \varepsilon \quad [3]$$

$$y = \beta_0 + \sum_{i=1}^k \beta_i x_i + \sum_{i=1}^k \beta_{ii} x_i^2 + \sum_i \sum_j \beta_{ij} x_i x_j + \varepsilon \quad [4]$$

In the above functions, β_0 is the constant value, β_i is the first-order (linear) coefficient, β_{ii} is the second-order (quadratic) coefficient, β_{ij} is the interaction coefficient, **k** is the number of independent variables, and ε is the rate of error.

In this research, the second-order model and Box-Behnken Design (BBD) are used. The software in use for experiment design and statistical analysis is Minitab [24]. Table 2 shows the design matrix with 46 tests in the form of coded runs. Five tests are repeated at the central levels of parameters (zero level).

2. 4. Experiment execution

An Al 1050-O sheet metal (annealed aluminum) was used in the experiments. The HLP68 grade hydraulic oil was used as lubricant [25]. The hemispherical-head tools were designed and manufactured in three diameters of 10, 15, and 20mm (Figure 2) in accordance with the instruction of design, manufacturing, and test of vibrating forming tools [17, 18]. Since the initial surface roughness of the sheet metal will influence the results, sheet metals with similar initial surface roughness were selected. Another effective factor was the surface quality of the forming tools, which were smooth and polished.

The ultrasonic equipment used in this research consists of two components: ultrasonic generator and ultrasonic vibration transmission

Table 2. Design matrix

Test no.	v	t	d	φ	f	Test no.	v	t	d	φ	f
1	0	0	-1	+1	0	24	0	0	0	0	0
2	0	0	+1	-1	0	25	0	-1	+1	0	0
3	0	0	-1	0	+1	26	0	+1	0	0	+1
4	0	+1	-1	0	0	27	+1	0	0	0	+1
5	0	0	0	0	0	28	+1	0	-1	0	0
6	0	0	0	0	0	29	+1	0	0	+1	0
7	-1	0	-1	0	0	30	-1	0	0	-1	0
8	0	0	0	+1	-1	31	0	0	0	0	0
9	0	+1	0	-1	0	32	0	+1	0	+1	0
10	-1	0	0	0	-1	33	+1	0	0	-1	0
11	0	0	0	0	0	34	0	0	0	-1	+1
12	0	+1	0	0	-1	35	+1	+1	0	0	0
13	-1	-1	0	0	0	36	-1	+1	0	0	0
14	0	-1	0	-1	0	37	0	+1	+1	0	0
15	0	0	-1	-1	0	38	0	-1	0	0	+1
16	+1	0	0	0	-1	39	0	0	+1	0	+1
17	0	0	0	-1	-1	40	-1	0	+1	0	0
18	0	0	0	+1	+1	41	+1	-1	0	0	0
19	0	0	-1	0	-1	42	-1	0	0	+1	0
20	0	-1	0	+1	0	43	0	-1	0	0	-1
21	0	-1	-1	0	0	44	0	0	+1	0	-1
22	+1	0	+1	0	0	45	-1	0	0	0	+1
23	0	0	+1	+1	0	46	0	0	0	0	0

system (piezoelectric transducer + tool holder). To apply ultrasonic vibration to the forming tool, a King generator with a power output of 1000 W at an operational frequency of 20 kHz was used. The ultrasonic generator converts low-frequency input voltage (220 VAC, 50-60 Hz) into high-frequency ultrasonic power (1000 W, 20 kHz). The vibration transmission system is combined with the forming tool, so that it can transfer the vibration energy efficiently to the sheet. In addition, the vibration transmission system must induce rotational movement of the forming tool (Fig. 3).

In this study, ultrasonic energy was applied longitudinally to the forming tool to be

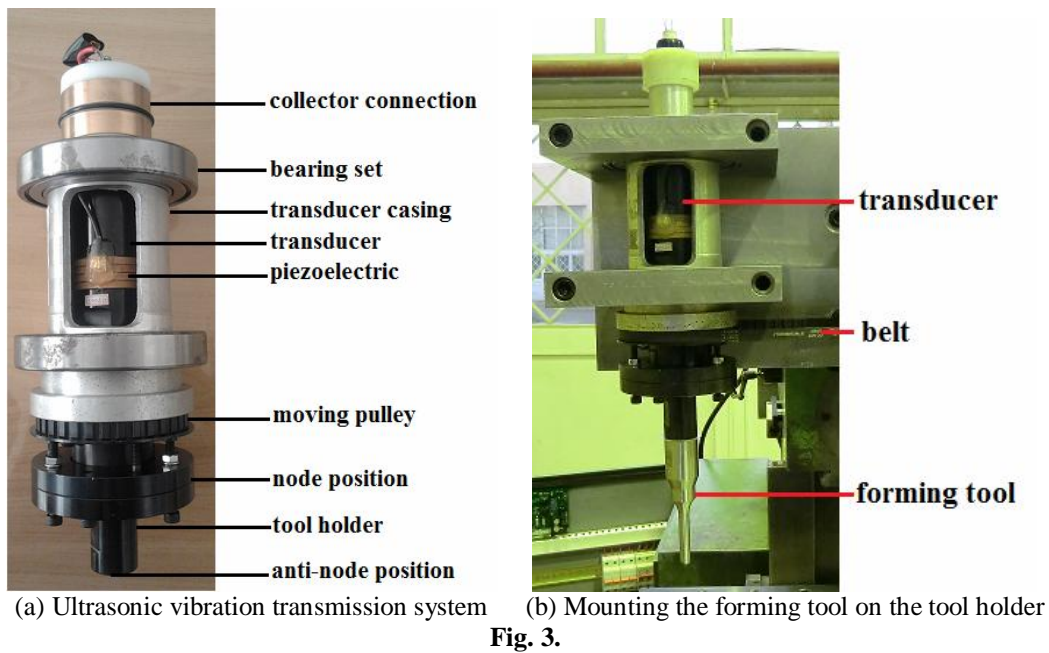
vibrated. To measure the nose vibration amplitude of the forming tool, a micron digital indicator was employed. The vibration amplitude of the forming tools was measured to be 7.5 μm . The spindle speed was 125 rpm.

Fig.4 shows the fixture components in the SPIF process. The sheet metal is placed between the clamping and backing plates. The sample geometry was considered in the form of pyramid frustum with the base dimension of 80 \times 80mm and depth of 30mm (Figure5).

Tool path strategy is in the form of the gradual imposing of the wall inclination angle (based on successive horizontal-vertical steps



Fig. 2. Vibrating forming tools



(a) Ultrasonic vibration transmission system

(b) Mounting the forming tool on the tool holder

Fig. 3.

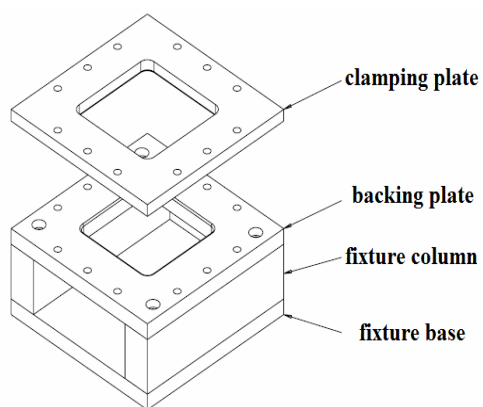


Fig. 4. Components of the fixture

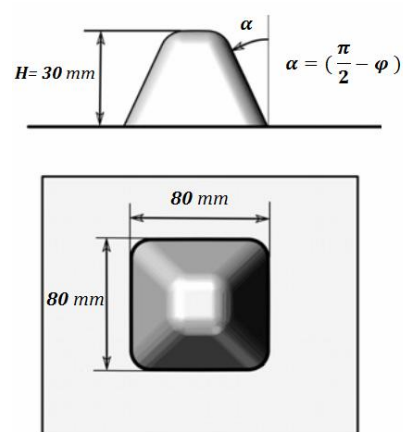


Fig. 5. Geometrical and dimensional characteristics of the specimen

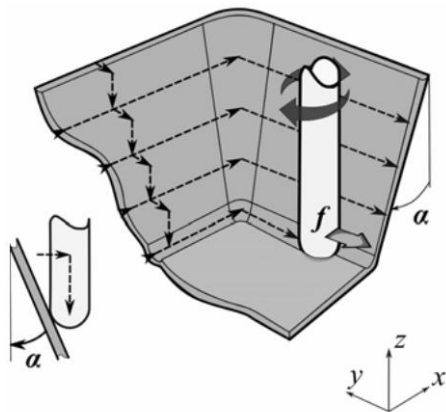


Fig. 6. Tool path strategy

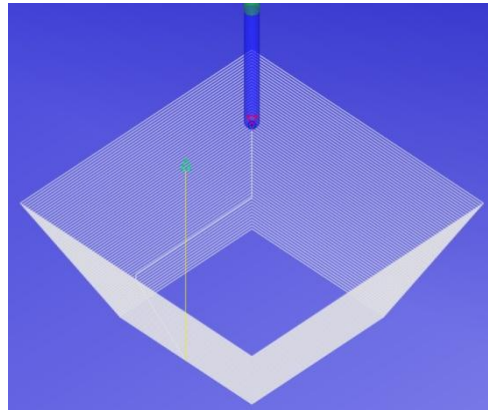


Fig. 7. Tool path simulation

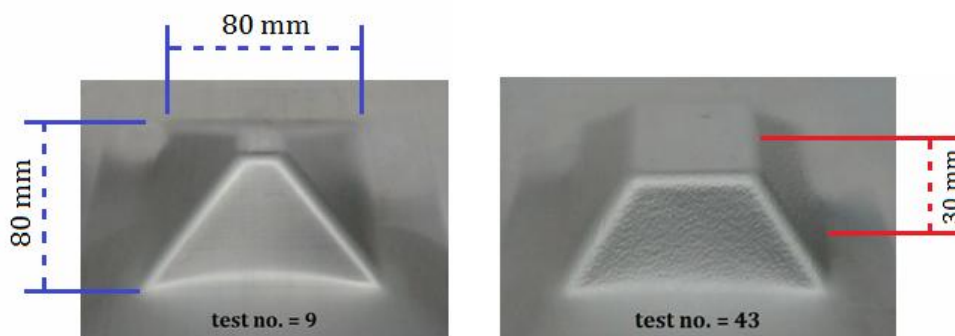


Fig. 8. Two formed samples in the experimental tests

in one face of the sample geometry) and then the linear motion in the working plane (Fig.6). Fig.7 shows the tool path simulation in Cimco software [26] for the wall inclination angle of $\varphi = 60^\circ$.

The tests were conducted in accordance with design matrix (Table 2) in a random order to avoid the effect of any errors occurred in the experiment. Experiments were performed using a CNC horizontal milling machine. The samples were formed in accordance with the concerned specifications. Fig. 8. shows the two specimens in the experimental tests.

2. 5. Measuring the response variable

The surface roughness was measured in three back faces of the samples (with the exception of the face related to the imposing of the tool penetration). The average of three measured values was registered as the mean value of the surface roughness. The plunger motion of the profilometer was performed in the central areas

of three faces and perpendicular to the tool path (Figure 9). Table 3 shows the results of measuring and calculation of the mean values of surface roughness.

2. 6. Data analysis

Analysis of the experimental data was performed by ANOVA. ANOVA is a powerful means to study the importance of a parameter and identify the significance of its effect. In addition, in order to create mathematical functions between the response variable and the effective parameters, the regression analysis was employed [21]. The confidence level (α) in the analysis was considered as equal to 0.05, which statistically means that the final model can predict the data with an error less than 5%. The effectiveness of a term is specified through **P-value**. Thus, the terms are identified with the $P\text{-value} \leq \alpha$, significant and with the $P\text{-value} > \alpha$ as insignificant. To the extent that the

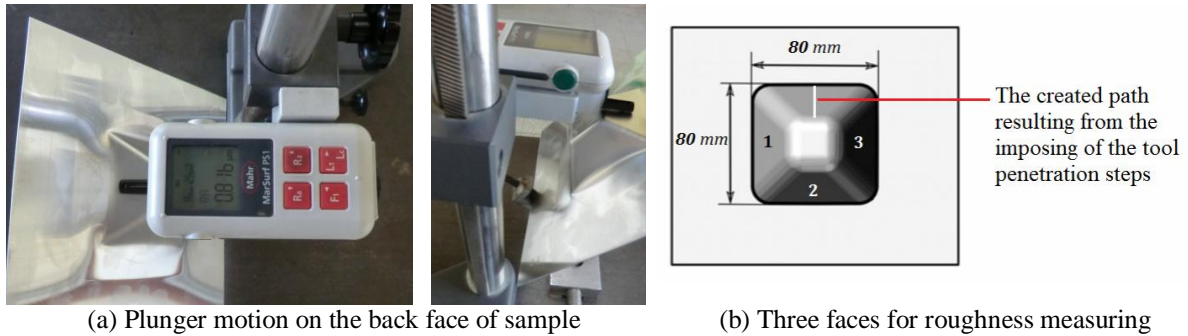


Fig. 9. Measuring procedure of the surface roughness

Table 3. Mean values of the surface roughness

Test no.	$R_z(\mu m)$	Test no.	$R_z(\mu m)$
1	2.91	24	2.60
2	2.00	25	5.87
3	2.98	26	2.20
4	3.03	27	3.67
5	2.50	28	4.89
6	2.52	29	3.55
7	1.68	30	1.63
8	2.13	31	2.61
9	2.79	32	2.07
10	1.60	33	4.39
11	2.53	34	2.73
12	2.32	35	3.86
13	5.68	36	1.60
14	6.43	37	1.90
15	3.17	38	6.18
16	3.92	39	1.84
17	2.81	40	1.51
18	2.01	41	7.40
19	3.13	42	1.53
20	6.06	43	6.37
21	6.90	44	1.98
22	3.36	45	1.55
23	1.81	46	2.72

P – value is smaller, to the same extent the significance of that term in the model is greater.

Thus, with the assumption of $\alpha = 0.05$ and

based on the primary results obtained from ANOVA, the first-order parameters: vertical step size (v), sheet thickness (t), tool diameter

Table 4. Regression table based on the effective terms

Term	Regression coefficient	T-value	P-value
Constant	2.547	77.335	0.000
v	1.141	37.049	0.000
t	-1.945	-63.142	0.000
d	-0.526	-17.084	0.000
φ	-0.243	-7.873	0.000
f	-0.069	-2.232	0.032
v × v	0.261	6.655	0.000
t × t	1.831	46.711	0.000
f × f	-0.106	-2.700	0.011
v × t	0.135	2.191	0.035
v × d	-0.340	-5.519	0.000
v × φ	-0.185	-3.003	0.005
$R^2 = 99.5$ $R_{adj}^2 = 99.4$			

(**d**), wall inclination angle (**φ**) and feed rate (**f**), the second-order terms: **v²**, **t²**, **f²** and interactional terms: **v.t**, **v.d** and **v.φ** were determined as the effective terms on the **R_z** and the other terms were determined as the ineffective terms.

In the final step of data analysis, the terms with inactive effects were removed from the model and only the terms with active effects were analyzed. Thus, all ineffective terms with the **P-value > 0.05** were deleted from the analysis and all terms with the **P-value ≤ 0.05** in the final step of ANOVA will be present. Table 4 shows the regression table resulting from the final ANOVA based on the effective terms. As can be observed, all the terms in Table 4 have appeared with the **P-value ≤ 0.05** and as the effective terms on the response variable. The emergence of positive sign (+) for regression coefficients states the presence of a direct relation between the terms and the response variable, whereas the emergence of negative sign (-) for regression coefficients shows the presence of a reverse relation between the terms and the response variable. In continuation, the role of

the effective parameters for achieving an ideal situation of the response variable was studied. Thus, the reduction of surface roughness (**R_z**) was determined as the ideal situation resulting from the UVaSPIF process.

The following relation expresses the regression equation of surface roughness as a function of the coded effective values:

$$R_z = 2.547 + 1.141v - 1.945t - 0.526d - 0.243\phi - 0.069f + 0.261v^2 + 1.831t^2 - 0.106f^2 + 0.135vt - 0.34vd - 0.185v\phi \quad [5]$$

The investigation of the T-values belonging to the effective terms shows that:

- Sheet thickness (**t**) as the linear effect has the greatest effect on **R_z**. On the other hand, the product of vertical step size and sheet thickness (**v.t**) as the interactional effect along with feed rate (**f**) as the linear effect has the least effect on **R_z**. In other words, the effect of sheet thickness (**t**) is 28 times more than the effect of **v.t** and feed rate.
- Sheet thickness (**t**) among the linear effects has the greatest effect on **R_z**.
- Sheet thickness (**t**) among the quadratic effects (**t²**) has the greatest effect on **R_z**.
- The product of vertical step size and tool diameter (**v.d**) among the interactional effects has the greatest effect on **R_z**.

As can be observed in Table 4, the correlation coefficients of **R²** and **R_{adj}²** show the highest values of 99.58% and 99.44%, respectively. As a result, a high correlation was established between the observed data in experimental tests and the predicted responses resulting from the regression equation. Hence, the ability of the fitted model and accuracy of the regression equation in describing and predicting the changes of the response variable were confirmed. Table 5 shows the results obtained from the ANOVA.

In order to investigate the accuracy of the regression model, in addition to **R²** evaluation, the lack-of-fit (LOF) test was also used. The significance of this test (**P-value_{LOF} ≤ 0.05**) indicates that the data are not well placed around the model and it is

Table 5. ANOVA results for the final model

Source of variation	Degree of freedom	Sum of squares	Mean squares	F-value	P-value
Regression	11	122.489	11.135	733.480	0.000
Linear	5	86.815	17.363	1143.690	0.000
v	1	20.839	20.839	1372.660	0.000
t	1	60.528	60.528	3986.950	0.000
d	1	4.431	4.431	291.870	0.000
φ	1	0.941	0.941	61.980	0.000
f	1	0.076	0.076	4.980	0.032
Square	3	35.002	11.667	768.510	0.000
v × v	1	0.000	0.672	44.290	0.000
t × t	1	34.891	33.125	2181.930	0.000
f × f	1	0.111	0.111	7.290	0.011
Interaction	3	0.672	0.224	14.760	0.000
v × t	1	0.073	0.073	4.800	0.035
v × d	1	0.462	0.462	30.460	0.000
v × φ	1	0.137	0.137	9.020	0.005
Residual Error	34	0.516	0.015	-	-
Lack-of-Fit	29	0.483	0.017	2.490	0.156
Pure Error	5	0.033	0.007	-	-
Total	45	123.005	-	-	-

not possible to use the model to predict the response variable. Thus, with the confirmation of the insignificance of the LOF test ($P - value_{LOF} > 0.05$), it is possible to find out that the model can be well fitted on the data. As can be observed in Table 5, the LOF test for the response variable is not significant and, consequently, the presented model shows the data trends well. On the other hand, the best analysis is performed when the regression is effective and the LOF test is ineffective concurrently [21]. Thus, with regard to the $P - value$, it is observed that the regression term is effective and the LOF term is ineffective.

The plot of normal probability is a useful means to check the accuracy of normal distribution of the residuals (Fig. 10). It is evident that residuals were scattered on the straight line and the errors have a normal distribution on the normal probability plot. Thus, the extracted regression model is adequate for the prediction of the effects. Also, it is possible to investigate the model

competency by studying the behavior of the residuals. The residual is defined in the form of the difference of the measured response in the experimental test and predicted response by the final model. If the regression model is suitable, then the residuals should be in lack of a structure. As can be seen in Fig. 11, the residuals have been distributed randomly around the zero axis and the diagram does not include any specific pattern. Thus, the final model is reliable and suitable.

The response behaviour can be shown in terms of the input variables in the form of 3D diagrams (surface plot) and 2D diagrams (contour plot). In these diagrams, the interactional effects of the two input variables on the response variable are observable and the values of other input variables are considered fixed at the central levels (zero level). The relationship of the surface roughness with the sheet thickness (t) and tool diameter (d) has been shown in Fig. 12. As can be observed, the increase of sheet thickness (t) along with the increase of tool diameter (d) is effective on the

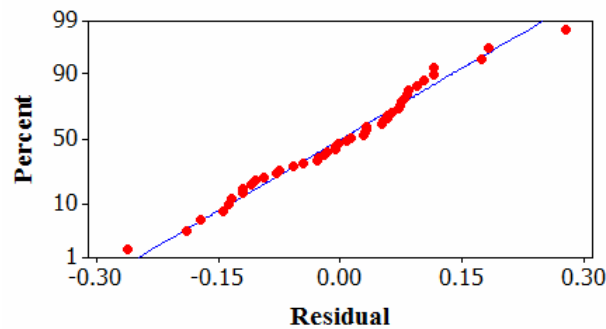


Fig. 10. Normal probability plot

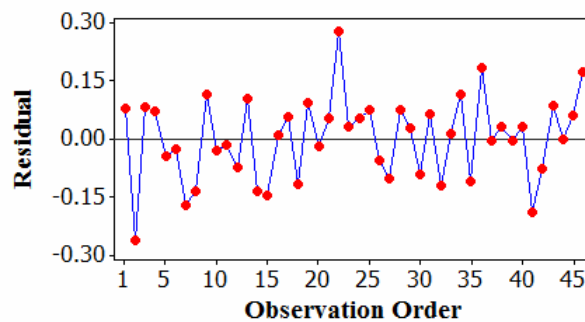


Fig. 11. The residual plot

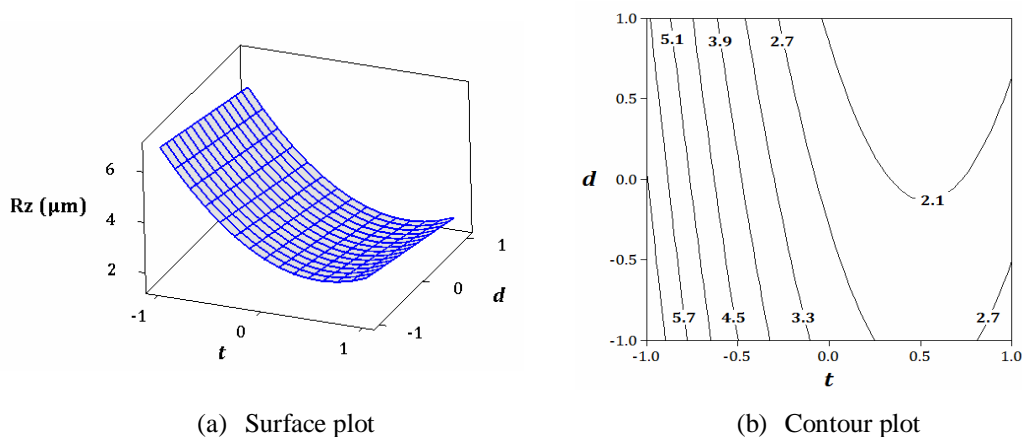


Fig. 12. Relationship of the surface roughness (R_z) with sheet thickness (t) and tool diameter (d)

reduction of the surface roughness of the specimen. On the other hand, the effect of wall inclination angle (ψ) on the reduction of surface roughness is insignificant in comparison with the effect of the increase of sheet thickness (t) (Figure 13).

2. 7. Optimization and confirmation

In this research, desirability method was used as the optimization technique due to its

simplicity, flexibility, and accessibility in the software. Drringer and Suich introduced this method in 1980 [27]. In this technique, the output response (y_i) is converted into dimensionless desirability of d_i ($0 < d_i < 1$), such that the higher value of d_i signifies the greater desirability of response value (y_i) and if the response is outside the acceptable limit, $d_i = 0$. Thus, for the output response, a separate desirability function with a range of 0

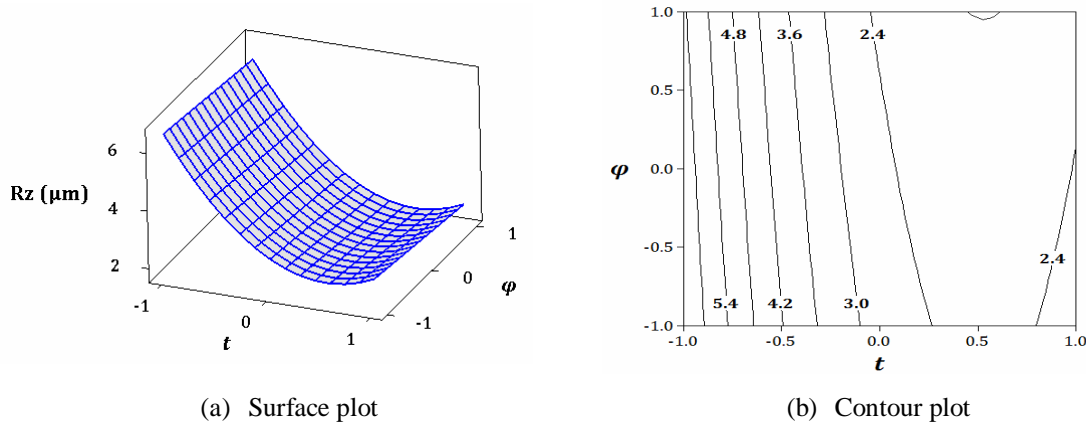


Fig. 13. Relationship of the surface roughness (R_z) with sheet thickness (t) and wall inclination angle (φ)

Table 6. Specifications of the desirability function

Output response	Desirability function	Function target	Weight value (r)
$y = R_z$	$d(y)$	$\text{Min}(R_z) = 1.51 \mu\text{m}$	1

<i>Optimal</i>	v	t	d	φ	f
D	1.0	1.0	1.0	1.0	1.0
1.0000	[-1.0]	[0.7071]	[-1.0]	[0.8384]	[-1.0]
<i>High</i>					
<i>Opt.</i>					
<i>Low</i>	-1.0	-1.0	-1.0	-1.0	-1.0

R_z					
Minimum					
$y = 1.2119$					
$d = 1.0000$					

Fig. 14. Behavior of the surface roughness (R_z) at the optimal points of input parameters

to 1 is obtained. In this research, the goal of the desirability function is the minimization of the response variable (reduction of surface roughness). Thus, desirability was defined in the following form:

$$d = \begin{cases} 1 & y < L \\ \left(\frac{U-y}{U-L}\right)^r & L \leq y \leq U \\ 0 & y > U \end{cases} \quad [6]$$

In the above relation, the L and U parameters are the low and high limits of response value (y), respectively. The shape of desirability function depends on the weight field (r) which is used to express the degree of significance of the target value. Here, the weight value was assumed equal to one ($r = 1$) and, consequently, the desirability function was defined in a linear mode. Table 6 shows the specifications of the desirability function for the output response.

Fig. 14 shows the diagrams of the surface roughness model resulted from the optimization process at the optimal point. As can be observed, the vertical line in red color shows the optimal values of input variables and the horizontal line in blue color shows the optimal value of output response. Thus, the effect of the input variables to achieve the target of desirability function is identifiable and interpretable from diagram simply.

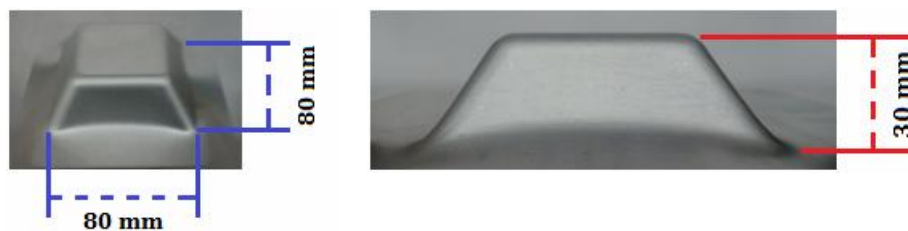
Table 7 shows the optimal values of the input variables to achieve the desirability function target. Therefore, the reduction of vertical step size (v), tool diameter (d) and feed rate (f) along with the increase of sheet thickness (t) and wall inclination angle (φ) lead to the reduction of surface roughness. As it is observed, the optimal angle of wall inclination (φ) was determined equal to 58.38° . Also, the optimal value of output response resulting from

Table 7. Optimal values of the input variables

Input variable	Coded optimal value	Actual optimal value
v	-1	0.25 mm
t	0.7071	0.91 mm
d	-1	10 mm
ϕ	0.8384	58.38°
f	-1	1500 mm/min

Table 8. Input variables for the confirmation test

variable	value
v	0.25 mm
t	0.9 mm
d	10 mm
ϕ	58°
f	1500 mm/min

**Fig. 15.** Formed sample in the confirmation test**Table 9.** Comparison between the results obtained from confirmation test and optimization process

R_z (confirmation test)	R_z (optimization process)	Difference percent
1.295 μm	1.212 μm	6.85 %

the regression equation is equal to 1.212 μm and the value of the corresponding desirability function is equal to one (1). Hence, with regard to the high value of separate desirability function, it can be claimed that the procedure of process optimization has well fulfilled a pre-determined target.

In order to confirm the optimized response and to measure the accuracy of the presented model, the experimental test was conducted by the optimal conditions of the input variables. Table 8 shows the input variables of the experiment. Fig. 15 shows the specimen after performing the confirmation test. Table 9 presents the results obtained from the confirmation test and its comparison with the optimized result. This comparison shows that the error of regression model to predict the surface roughness is less than 7%. Thus, the accuracy and preciseness of regression model

to predict the response variable was confirmed.

3. Conclusion

In this paper, analysis and optimization of the surface roughness in the UVaSPIF process were conducted based on DOE principles using the RSM technique. The major accomplishments of this research are summarized as follows:

- The primary results obtained from ANOVA with the assumption of $\alpha = 0.05$ showed that the linear terms: vertical step size (v), sheet thickness (t), tool diameter (d), wall inclination angle (ϕ) and feed rate (f), the quadratic terms: v^2 , t^2 and f^2 and the interactional terms: $v.t$, $v.d$ and $v.\phi$ can affect the surface roughness.
- The regression equation resulting from ANOVA was extracted to predict the surface roughness in the UVaSPIF process. The

competency of the final model was investigated by the correlation coefficients, lack-of-fit (LOF) test, normal probability plot, and residuals diagram. Consequently, the ability of the fitted model and the accuracy of the regression equation in describing and predicting the behavior of surface roughness were confirmed.

- With regard to the comprehensiveness of the presented mathematical model in this research, a broad range of effective factors on the surface roughness was covered. Thus, the presented model can be utilized in different methods of incremental forming in addition to prediction and control of surface roughness parameter in UVaSPIF process.
- The optimal values of input variables were extracted to access the least surface roughness. The optimization results indicated that the reduction of vertical step size, tool diameter, and feed rate along with the increase of sheet thickness and wall inclination angle lead to the reduction of surface roughness. Also, the optimal angle of wall inclination was determined as equal to 58.38°.
- The high value of the desirability function corresponding to the surface roughness ($d = 1$) showed that the optimization procedure has successfully fulfilled a pre-determined target.
- A comparison between the results obtained from the confirmation test and optimization procedure showed that the error of regression model for prediction of surface roughness is less than 7%. Thus, the accuracy and preciseness of regression model to predict the surface roughness was confirmed.

Acknowledgements

The corresponding author would like to thank Dr. Abrinia and Dr. Abdullah for their sincere support of this project.

References

1. B. V. Desai, K. P. Desai, H. K. Raval, "Die-Less rapid prototyping process: Parametric investigations", *Procedia Materials Science*, Vol. 6, 2014, pp. 666-673.
2. B. S. Raju, U. Chandra Shekar, K. Venkateswarlu, D. N. Drakashayani, "Establishment of process model for rapid prototyping technique (Stereolithography) to enhance the part quality by Taguchi method", *Procedia Technology*, Vol. 14, 2014, pp. 380-389.
3. V. Jaiganesh, A. C. Andrew, E. Mugilan, "Manufacturing of PMMA cam shaft by rapid prototyping", *Procedia Engineering*, Vol. 97, 2014, pp. 2127-2135.
4. P. Jain, A. M. Kuthe, "Feasibility study of manufacturing using rapid prototyping: FDM approach", *Procedia Engineering*, Vol. 63, 2013, pp. 4-11.
5. E. Leszak, "Apparatus and process for incremental dielessforming", US Patent No. 3342051A, 1967.
6. K. Kitazawa, A. Wakabayashi, K. Murata, K. Yaejima, "Metal-flow phenomena in computerized numerically controlled incremental stretch-expanding of aluminium sheets", *Keikinzoku J. Jpn. Inst. Light Met.*, Vol. 46, 1996, pp. 65-70.
7. A. Petek, B. Jurisevic, K. Kuzman, M. Junkar, "Comparison of alternative approaches of single point incremental forming processes", *Journal of Materials Processing Technology*, Vol. 209, 2009, pp. 1810-1815.
8. J. Duflou, Y. Tunckol, A. Szekeres, P. Vanherck, "Experimental study on force measurements for single point incremental forming", *Journal of Materials Processing Technology*, Vol. 189, 2007, pp. 65-72.
9. J. Jeswiet, F. Micari, G. Hirt, A. Bramley, J. Duflou, J. Allwood, "Asymmetric single point incremental forming of sheet metal", *Ann. CIRP*, Vol. 54, No. 2, 2005, pp. 623-649.
10. S. Thibaud, R. BenHmida, F. Richard, P. Malécot, "A fully parametric toolbox for the simulation of single point incremental sheet forming process: Numerical feasibility and experimental validation", *Simulation Modelling Practice and Theory*, Vol. 29, 2012, pp. 32-43.
11. B. Lu, J. Chen, H. Ou, J. Cao, "Feature-based tool path generation approach for incremental sheet forming process", *Journal of Materials Processing Technology*, Vol. 213, 2013, pp. 1221-1233.
12. B. Lu, Y. Fang, D. K. Xu, J. Chen, H. Ou, N. H. Moser, J. Cao, "Mechanism investigation of friction-related effects in single point incremental forming using a developed oblique roller-ball tool", *International Journal of Machine Tools & Manufacture*, Vol. 85, 2014, pp. 14-29.

13. S. Junk, G. Hirt, I. Chouvalova, "Forming strategies and tools in incremental sheet forming", Proceedings of the 10th International Conference on Sheet Metal, 2003, pp. 57-64.
14. E. Hagan, J. Jeswiet, "Analysis of surface roughness for parts formed by computer numerical controlled incremental forming", Journal of Engineering Manufacture (Part B), Vol. 218, 2004, pp. 1307-1312.
15. M. Durante, A. Formisano, A. Langella, "Comparison between analytical and experimental roughness values of components created by incremental forming", Journal of Materials Processing Technology, Vol. 210, 2010, pp. 1934-1941.
16. S. P. Shanmuganatan, V. S. Senthil Kumar, "Metallurgical analysis and finite element modelling for thinning characteristics of profile forming on circular cup", Materials and Design, Vol. 44, 2013, pp. 208-215.
17. M. Vahdati, R. A. Mahdavejad, S. Amini, A. Abdullah, K. Abrinia, "Design and Manufacture of Vibratory Forming Tool to Develop Ultrasonic Vibration assisted Incremental Sheet Metal Forming Process", Modares Mechanical Engineering, Vol. 14, No. 11, 2014, pp. 68-76 (In Persian).
18. M. Vahdati, R. A. Mahdavejad, S. Amini, K. Abrinia, "Experimental investigation the effect of ultrasonic vibration and lubricant on behavior of the forming force in Single Point Incremental Forming (SPIF) process", 3rd International Engineering Materials & Metallurgy Conference, Iran, 2014, p. 159.
19. M. Moradi, M. Ghoreishi, J. Frostevar, A. F. H. Kaplan, "An investigation on stability of laser hybrid arc welding", Optics and Lasers in Engineering, Vol. 51, No.4, 2013, pp. 481-487.
20. H. Abdollahi, R. A. Mahdavejad, M. Ghambari, M. Moradi, "Investigation of green properties of iron/jet milled grey cast iron compacts by response surface method", Journal of Engineering Manufacture (Part B), Vol. 228, No. 4, 2014, pp. 493-503.
21. D. C. Montgomery, "Design and Analysis of Experiments", 3rd ed., New York, John Wiley & Sons, 1991.
22. A. I. Khuri, J. A. Cornell, "Response Surfaces Design and Analysis", 2nd ed., New York, Marcel Dekker, 1996.
23. R. H. Myers, D. C. Montgomery, "Response Surface Methodology: Process and Product Optimization Using Designed Experiments", 2nd ed., New York, John Wiley & Sons, 2002.
24. "Minitab software", release 16, <http://www.minitab.com>.
25. "DIN 51524", Part 2.
26. "CIMCO software", <http://www.cimco.com>.
27. R. H. Myers, D. C. Montgomery, C. M. Anderson-Cook, "Response Surface Methodology: Process and Product Optimization Using Designed Experiments", 3rd ed., New York, John Wiley & Sons, 2009.